Properties of the D_1 bound exciton in 4H-SiC

T. Egilsson,* J. P. Bergman, I. G. Ivanov, A. Henry, and E. Janzén
Department of Physics and Measurement Technology, Linköping University, S-581 83 Linköping, Sweden
(Received 23 March 1998)

In this paper we report an extensive study of the properties of the D_1 photoluminescence (PL) observed in electron irradiated 4H-SiC. We have investigated the temperature dependence of the PL, its time decay and excitation properties. At low temperatures ($T<5$ K) the D_1 PL spectrum in 4H-SiC consists of one no-phonon line, L_1 (4272.6 Å), and its phonon replicas. As the temperature is raised, two higher energy no-phonon lines, M_1 (4261.3 Å) and H_1 (4257.0 Å), appear while the L_1 intensity rapidly decreases. At sufficiently high temperatures ($T>100$ K) the D_1 PL is quenched. The associated activation energy is found to be approximately 57 meV. The lifetime of the D_1 PL is around 450 μs at 1.3 K, but decreases to 2 μs at 70 K. At high temperatures the time decay of the three lines, L_1, M_1, and H_1, is identical, showing that they are thermalized. PL excitation (PLE) spectra of phonon replicas of the L_1 line at low temperature reveal a weak peak corresponding to the L_1 no-phonon line and two strong peaks corresponding to the M_1 and H_1 lines. We also notice a weak peak, N_1, about 0.5 meV above the M_1 line. Furthermore, there is a series of sharp lines at higher energies in the PLE spectra. The energy positions of these lines can be fitted by a hydrogenic series of excited states with an associated binding energy of 53 meV. Our results can be explained by exciton recombination at an isoelectronic center. One of the particles of the exciton is weakly bound, whereas the other is more tightly bound. [S0163-1829(99)00803-6]

I. INTRODUCTION

The physical properties of silicon carbide (SiC) make the material well suited for high-temperature, high-power, and high-frequency electronics. The recent progress in crystal growth of SiC has led to an increased interest in its development. SiC exists in several different polytypes of which the 3C, 4H, 6H, and 15R polytypes are the most common. Of these, the 4H polytype is considered to be the most appropriate for high-power applications, as it has the widest band gap and an almost isotropic electron mobility.[1] Very high temperatures (>1800 °C) are needed for diffusion doping of SiC,[2] making the method impractical. Therefore, doping by ion implantation is of major importance. The main problem concerning ion implantation is the damage it causes to the lattice. This gives rise to unwanted defects that can be detrimental to device performance. Some of these can be removed by thermal annealing but others persist even at very high temperatures. The D_1 center is the best known example of the latter type of defect in SiC. Its fingerprint is an efficient luminescence of energy 0.35–0.45 eV below the excitonic band gap, composed of sharp no-phonon lines followed by a characteristic phonon-assisted structure. It has been observed in the polytypes 3C-, 4H-, 6H-, 15R-, and 21R-SiC (see Ref. 3 and references therein) and after various kinds of bombardment. It has also been observed in as-grown material after quenching from the growth temperature.[3] The most detailed investigations of the D_1 photoluminescence (PL) have been carried out for the 3C, 6H, and 15R polytypes. These consist of temperature-dependent PL measurements for the three polytypes (Refs. 4–6) and Zeeman spectroscopy for 6H-SiC.[7] In the 6H polytype the PL decay times at 10 and 77 K have also been determined.[7] Furthermore, some absorption and excitation spectra were reported for 3C- and 6H-SiC.[8]

The D_1 PL exhibits a complicated temperature dependence. Depending on the SiC polytype, the spectra are composed of either two or three superimposed spectra. The subspectra consist of a polytype dependent number (n) of no-phonon lines, each accompanied by the characteristic D_1 phonon structure. At the lowest temperatures, the lowest-energy subspectrum dominates, but as the temperature increases the higher-energy subspectra take over. The letters L, M, and H (low, medium, and high temperature) are used to label the different subspectra. The no-phonon lines are denoted by L_i, M_i, and H_i where i runs from 1 to n. In the case of 3C-SiC there are three subspectra (L, M, and H) and n is equal to 1.[4] For 6H-SiC and 15R-SiC there are only two subspectra (L and H) and n is equal to 3 and 4, respectively.[5,6]

The properties of the D_1 PL are rather characteristic of excitonic decay at isoelectronic defects. The large binding energy indicates binding by short-range forces to uncharged centers according to experience with other semiconductors.[9] The long lifetime of the luminescence [150 μs at 10 K for L_1 and 1 μs at 77 K for H_1 in 6H-SiC (Ref. 7)] indicates that there is no competing Auger process and that the binding center is therefore most probably isoelectronic. The appearance of low- and high-temperature forms of the spectra is also typical, as the ground state of the exciton splits due to exchange coupling between the electron and the hole. When exchange coupling between the two particles is strong, this tends to lead to an almost forbidden low-energy transition and a higher-energy allowed transition.[9] This can explain the different temperature behavior of the low- and high-energy lines as well as the change in lifetime.

Measurements of the Zeeman splitting of the L_i and H_i lines in 6H-SiC showed that the former consist of five components but the latter do not split.[7] Extrapolation of the Zeeman splitting of the L_i lines to zero field indicates a small

zero field splitting of about 0.3 meV. In analogy with the commonly used treatment of excitons at isoelectronic centers in cubic semiconductors, Dean, Bimberg, and Choyke (Ref. 7) interpreted the data within the framework of a J-J coupling model, adding a uniaxial crystal field as a perturbation. The L_i lines were associated with dipole forbidden $J=2$ to $J=0$ transitions and the H_i lines with dipole allowed $J=1$ to $J=0$ transitions. Arguments favoring a tightly bound electron and a weakly bound hole were presented. However, it is worth pointing out here that the J-J coupling scheme is questionable in the case of a uniaxial crystal such as 6H-SiC due to the large crystal field splitting of the valence band and relatively small spin-orbit coupling. A satisfactory explanation of the Zeeman results therefore still remains to be given. The D_1 PL is not seen to depend on any specific impurities. This is judged from its independence of the implanted ion in material damaged by ion implantation, and its independence of the impurity content of the samples.[10] The D_1 PL intensity increases with annealing up to high temperatures ($\sim$1700 °C) but is destroyed by annealing beyond that. The defect is therefore thought to be a complex.[10]

In this paper we present an investigation of the optical properties of the D_1 center observed in electron irradiated 4H-SiC. Previous work on the D_1 PL in 4H-SiC is very scarce. In the first report,[11] the PL measurements were limited to 80 K so only the high-temperature form of the spectrum was observed. More recently the low-temperature PL spectrum has been reported.[12–14] These reports do not agree on the number of D_1 related lines, however. In one of them (Ref. 12) two low-temperature no-phonon lines L_1 (4274.0 Å) and L_2 (4311.6 Å) are associated with the D_1 center. In the others, only one D_1 related line, namely, L_1 (4272 Å), was observed. The spectra shown in Ref. 14 do, however, contain a line at around 4311 Å but it is seen to have a completely different thermal stability than the D_1 L_1 line. The authors speculate that this is the L_2 line observed in Ref. 12 and reject its presumed relation to the D_1 defect.

The SiC polytypes have different numbers of inequivalent lattice sites. For a single-site optically active center the inequivalent sites usually give rise to PL lines of different energy. If a center contains more than one lattice site the situation is more complicated. The number of inequivalent centers within a particular polytype will then depend on the structure of the defect. In 3C- and 6H-SiC the number of no-phonon lines within each subspectrum of the D_1 PL is equal to the number of inequivalent substitutional sites.[4,5] But for 4H-, 15R-, and 21R-SiC the number of these lines is one less than the number of nonequivalent substitutional sites.[6,11]

The paper is organized as follows: (i) In Sec. II we describe the samples and experimental details; (ii) Sec. III A presents the low-temperature PL spectrum of the D_1 center in 4H-SiC; (iii) in Sec. III B the temperature dependence of the PL is shown; (iv) Sec. III C presents the time resolved PL results; (v) Sec. III D deals with the PL excitation (PLE) results; (vi) finally, in Sec. IV we give a summary and our main conclusions.

II. EXPERIMENT

The 4H-SiC samples used for the investigation were high-quality 30–40-μm-thick epitaxial layers grown by chemical vapor deposition on n^+ [0001] oriented substrates with an off-axis cut of 8°. The residual doping of the layers was in the low 10^{14} cm^{-3} range. The samples were irradiated by a dose of 10^{17} cm^{-2} of 2 MeV electrons and then annealed at 1500 °C for 1 h. The damage caused by the irradiation is expected to be approximately uniform throughout the entire thickness of the samples.

For the optical experiments, He bath cryostats with facilities for temperature variation were used. We used either the 244-nm line of a frequency-doubled Ar-ion laser or the 334-nm line of a standard Ar-ion laser for the PL measurements. For the PLE and selectively excited PL measurements we used blue light from a dye laser pumped with the multiline UV of an Ar-ion laser. The time-resolved PL measurements were performed using a frequency-tripled diode pumped YAG laser with a variable repetition frequency 0.1–50 kHz, and an excitation wavelength of 355 nm. For all of the PLE measurements and some of the low-temperature PL measurements the luminescence was dispersed by a 0.85-m SPEX 1404 double grating monochromator fitted with 1800 grooves/mm gratings and detected by a Hamamatsu photomultiplier tube (PMT) operating in photon counting mode. The temperature-dependent PL was recorded by a liquid-nitrogen cooled charge-coupled device (CCD) camera attached to a single grating Jobin-Yvon monochromator fitted with a 2400 grooves/mm grating. For time-resolved measurements the PL was dispersed through a single grating monochromator and detected with a photon counting PMT, where the pulses were collected with a multichannel photon counter. The time resolution of the system is limited by the pulse width of the YAG laser, which is less than 50 ns.

Most of the PL measurements were carried out in a near backscattering configuration. However, in order to determine the polarization of the D_1 no-phonon lines we also measured the PL through a cleaved edge while exciting through the surface. PL contribution from the surface region was avoided by placing a barrier of silver paste close to the sample edge. The spectra were corrected for the wavelength-dependent polarization effect of the monochromator. The PLE spectra were taken by monitoring the L_1 no-phonon line (or one of its replicas) by a double-grating monochromator while scanning the dye laser excitation above (or across) the no-phonon line. Although it is the linewidth of the dye laser line ($<$0.2 Å in our case) that determines the resolution of the PLE spectra, we found it advantageous to limit the slit widths of the monochromator to 200 μm in order to reduce the effects of stray light. This also allows us to restrict the excitation spectra to a certain sharp PL line. With the above-mentioned slit widths our monochromator has a resolution of approximately 0.6 Å. The output power of the dye laser is not constant over the entire wavelength region of interest. Its dependence on the wavelength is smooth, however, and has been taken into account in the PLE spectra shown in this paper. Selectively excited PL spectra were taken by adjusting the dye laser excitation wavelength to one of the PLE peaks and then recording the PL. As the detection wavelength lies close to the excitation wavelength in these experiments the spectra can be influenced by Raman lines. The Raman peaks were easily identified by their shift and approximately constant intensity when shifting the detection (excitation) wavelength in PLE measurements (selectively excited PL measure-

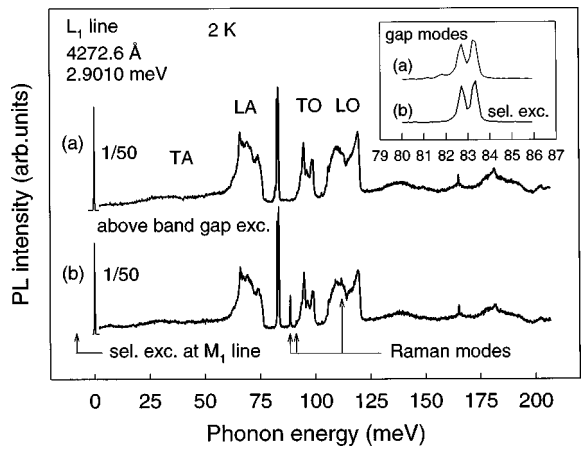

FIG. 1. PL spectra excited with (a) above band gap light (244 nm) and (b) subband-gap light. In (b) the PL spectrum was selectively excited with the light of energy coinciding with the next-lowest energy level of the D_1 exciton, M_1 (4261.3 Å, 2.9087 eV). Both spectra were recorded at 2 K. The inset shows an enlargement view of the phonon gap modes.

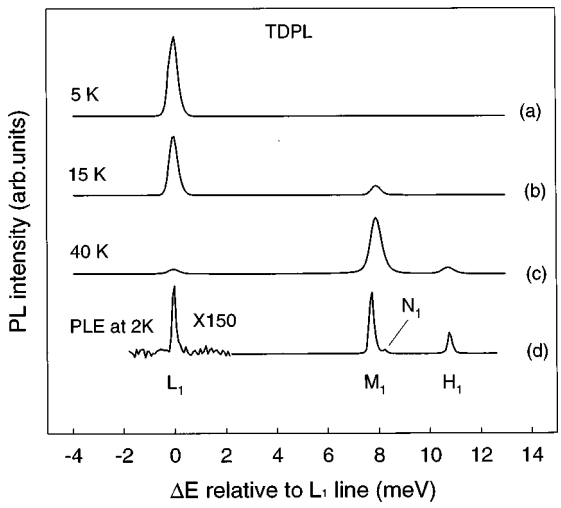

FIG. 2. Temperature dependence of the no-phonon part of the D_1 PL. The spectra in (a), (b), and (c) show how the PL gradually moves from the L_1 line to the M_1 and H_1 lines with increasing temperature. (d) is the PLE spectrum of the 82.7-meV phonon replica of the L_1 line, taken at 2 K.

ments). We used the characteristic 4H-SiC Raman modes at 776 cm^{-1} (96.2 meV) and 796 cm^{-1} (98.7 meV) as reference lines for the calibration of our spectra. The Raman mode at around 963 cm^{-1} (119 meV) was also observed but is less reliable as a reference since its exact position depends on sample doping.[15] We will refer to these Raman lines as R_1, R_2, and R_3, respectively.

III. RESULTS

A. Low-temperature photoluminescence

The D_1 low-temperature PL observed in 4H-SiC consists of a single no-phonon line L_1 at 4272.6 Å (2.9010 eV) and its phonon replicas. The linewidth of L_1 in our samples at 2 K is approximately 0.3 meV. In Fig. 1(a) we show a PL spectrum excited with above band-gap light (244 nm) and in Fig. 1(b) a PL spectrum selectively excited with sub-band-gap light of energy coinciding with the next lowest energy level of the D_1 exciton M_1 (4261.3 Å, 2.9087 eV). In the case of the selective excitation, absorption into the energy state M_1 is used to feed the L_1 PL. This is possible as the exciton created in the M_1 state relaxes at this low temperature to the lowest-energy L_1 state before it has a chance to recombine. The main difference between the two spectra is the presence of the R_1, R_2, and R_3 Raman lines (see Sec. II) that show up in the selectively excited PL spectrum. Apart from one minor discrepancy to be discussed later, the PL's in the two spectra are identical. It is therefore clear that the luminescence in the above-band-gap excited spectra is due almost entirely to the D_1 PL. The phonon structure is similar to that of the D_1 PL in the 3C and 6H polytypes. The broader features have been explained in terms of coupling to TA, LA, TO, and LO lattice modes.[4,5] In addition to the lattice phonon replicas there are three sharp lines at 82.7, 83.4, and 165.2 meV from the no-phonon line. The first two modes lie in the forbidden gap of lattice modes and are therefore assigned to localized modes. The line at 165.2 meV is most probably a two-phonon mode since its energy is very close to twice that of the 82.7-meV mode and its intensity is relatively low. The slight discrepancy between the two spectra in Fig. 1 mentioned previously is the two small bumps just to the left of the gap modes (see inset in Fig. 1) in the above-band-gap excited PL spectrum. No corresponding peaks were observed to the left of the no-phonon line. We observed these small peaks repeatedly in our above-band-gap excited D_1 PL spectra irrespective of the particular sample or the precise experimental conditions. On the other hand, they were never seen in the selectively excited PL spectra. The peaks may be due to PL excited by the above-band-gap light but unrelated to the D_1 PL.

B. Temperature-dependent photoluminescence

Figure 2 shows the dependence of the no-phonon part of the D_1 PL of 4H-SiC on temperature. In order to concentrate on the main thermally induced changes we plot only the low- (a), medium- (b), and high- (c) temperature cases. At low temperature (a) only the L_1 line is visible. At medium temperatures (b) the L_1 intensity decreases and another line M_1 at higher energy appears. At higher temperatures the M_1 line rapidly takes over the spectrum and the highest-energy no-phonon line H_1 appears (c). Further increase of the temperature leads to broadening of the lines, and a slight shift to lower energies due to the lowering of the band gap. Finally, at temperatures between 100 and 250 K the D_1 PL quenches. The polarization of the three no-phonon lines L_1, M_1, and H_1 is shown in Fig. 3. The measurement procedure is described in the experimental section. All the lines are predominantly polarized perpendicular to the c axis. According to the model of Dean, Bimberg, and Choyke,[7] based on Zeeman results on 6H-SiC, the D_1 exciton should have two high-energy lines, one polarized parallel to the crystal c axis, and the other polarized perpendicular to the c axis. This model does not fit our results. Figure 4 shows an Arrhenius plot of the temperature dependence of the intensity of the L_1, M_1, and H_1 no-phonon lines from 15 to 250 K. The intensity of the lines was estimated by taking the product of

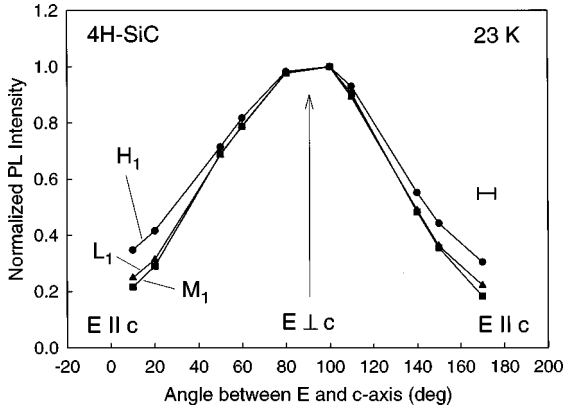

FIG. 3. Polarization dependence of the L_1, M_1, and H_1 lines. The intensities are normalized. The error bar shown in the left part of the figure indicates the estimated accuracy of the angle measurement.

the peak height and the peak width at half-maximum. The inset of the figure shows the Arrhenius plot of the M_1/L_1 and H_1/L_1 intensity ratios below 70 K. The ratios are well described by Boltzmann statistics, and fitting gives $M_1/L_1 = 135\exp(-8\ \text{meV}/kT)$ and $H_1/L_1 = 65\exp(-11\ \text{meV}/kT)$. The energy values are in good agreement with the energy separation of the PL lines, 7.7 and 10.7 meV (see Fig. 2). At temperatures above 100 K it is not possible to distinguish between the M_1 and H_1 lines as they merge due to the line broadening at these high temperatures. The continuation of the M_1 points above 100 K on the plot therefore contains the joint intensity of the M_1 and H_1 lines. This represents the total intensity of the no-phonon part of the D_1 PL since the L_1 line intensity is negligible at high temperatures. The thermal activation energy (E_a) calculated from the quenching of the D_1 no-phonon PL at high temperatures (see Fig. 4) is approximately 57 meV. Here, we have not taken into account

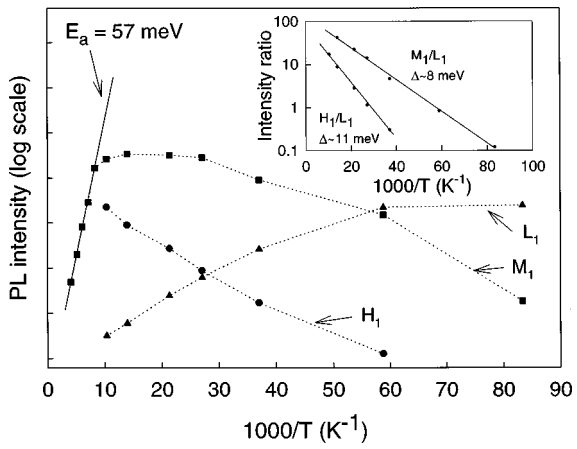

FIG. 4. Arrhenius plot of the temperature dependence of the intensity of the L_1, M_1, and H_1 no-phonon lines from 15 to 250 K. The five leftmost points are the combined intensity of the M_1 and H_1 lines. The thermal activation energy $E_a = 57$ meV is calculated from the slope of the linear fit to these five leftmost points. The inset shows Arrhenius plots for the intensity ratios M_1/L_1 and H_1/L_1 at temperatures between 15 and 70 K. The activation energies, labeled Δ, found from the linear fits agree well with the separation of the relevant no-phonon lines in the PL spectra.

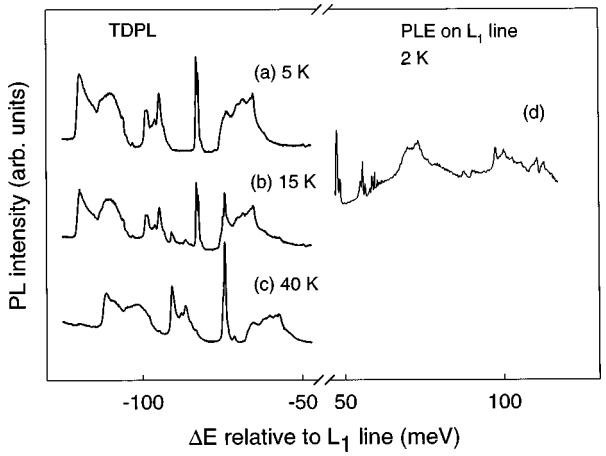

FIG. 5. The spectra in (a), (b), and (c) show the phonon part of the D_1 PL at different temperatures. The spectrum in (d) shows the high-energy part of the PLE spectrum of the L_1 no-phonon line at 2 K.

the contribution of the phonon-assisted transitions to the D_1 PL intensity. This means that we assume the phonon coupling of the M_1 and H_1 states to be constant in the temperature range 100–250 K. The excitonic band gap E_{gx} of 4H-SiC at 4.2 K is 3.266 eV.[16] The energies of the M_1 and H_1 lines at this temperature are 2.9087 and 2.9118 eV, respectively, which gives binding energies of approximately 356 and 353 meV with respect to E_{gx}. For comparison with the thermal activation energy we need to add to this the free-exciton binding energy, which has been estimated to be approximately 20 meV (Ref. 17) in 4H-SiC. There is obviously a large discrepancy between the thermal activation energy and the localization energy of the D_1 exciton. This can be explained by weak binding of one of the excitonic particles as compared to the other. It means that the exciton luminescence is quenched by thermal release of the weakly bound particle while the other remains bound at the center. This is consistent with the Hopfield-Thomas-Lynch model of excitons bound to isoelectronic centers.[18] An alternative explanation is the thermal activation of a competing recombination channel for the excited carriers. In a later section we present experimental results that strongly support the former possibility. The temperature dependence of the main part of the D_1 phonon structure is shown in Fig. 5. If the curve at 5 K where only the L_1 phonon spectrum appears is compared to the curve at 40 K where the M_1 phonon spectrum dominates, it can be seen that the phonon structure accompanying these no-phonon lines is very similar. The only obvious difference is the change in relative intensity of the two gap modes and the increased intensity of the low energy part of the TO band at high temperatures. The curve at 15 K shows the transition between the two spectra. We are not able to distinguish clearly the phonon spectra accompanying the H_1 line as it is always overlapped by the stronger M_1 spectrum.

C. Time-resolved photoluminescence

The time decay of the L_1, M_1, and H_1 lines was measured as a function of temperature. The decay is a simple exponential, except at temperatures below approximately 3 K, where a faster component superimposed on the slow ex-

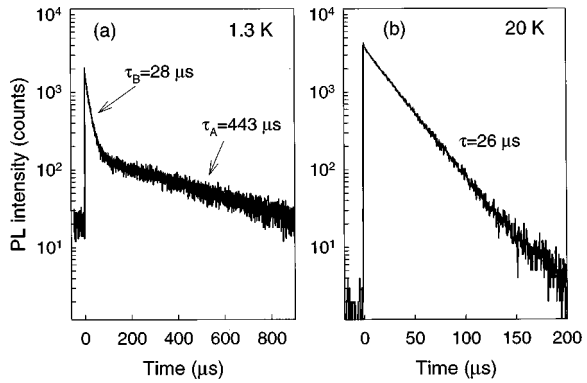

FIG. 6. PL decay curves of the L_1 line at (a) 1.3 K and (b) 20 K. At 1.3 K there are clearly two components with associated lifetimes τ_A and τ_B, whereas there is only one at 20 K.

ponential decay can be resolved. When possible, the PL decay was measured separately on each of the three lines. Their PL decay was found to be identical, which shows that the associated states are thermalized. However, at the lowest temperatures (<15 K) only the L_1 decay could be measured due to the low intensities of the M_1 and H_1 lines. Figure 6 shows the PL decay curves of the L_1 line at (a) 1.3 K, and (b) 20 K. At 1.3 K there are clearly two components with associated lifetimes τ_A and τ_B, whereas there is only one at 20 K. In Fig. 7 the decay lifetime is plotted as a function of temperature. The lifetime changes most rapidly between 1.3 and 4.2 K, and between 15 and 70 K. We explain the decreased lifetime at high temperatures by the increased population of the M_1 and H_1 levels. From the temperature-dependent PL measurements discussed in a previous section we found that the M_1 and H_1 levels have much higher oscillator strengths than the L_1 level. This also means that they decay faster than L_1. In order to explain the decrease of the lifetime at low temperatures, we assume a small splitting of the L_1 state into two substates, the lower one, L_{1A}, having longer lifetime than the upper one, L_{1B}. Splitting of the D_1 exciton low-energy state has previously been deduced from extrapolation of the L_1 line Zeeman splittings in 6H-SiC to

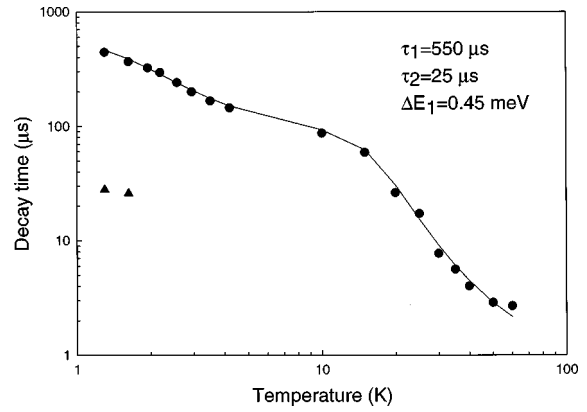

FIG. 7. Temperature dependence of the lifetime of the D_1 PL no-phonon lines in 4H-SiC. The triangular points show the lifetime of the fast component, only observed at the lowest temperatures. The solid curve in the figure shows a fit taking into account four levels, two closely spaced levels at low temperature, L_{1A} and L_{1B}, and the two high-temperature levels M_1 and H_1.

zero field.[7] The splitting derived from the Zeeman measurements indicated a central singlet in between two doublets split off from the central line by approximately 0.3 meV. The solid curve in Fig. 7 shows a fit taking into account four levels, two at low temperature (L_{1A} and L_{1B}) and two at high temperature (M_1 and H_1) assuming thermal equilibrium. The formula used is

$$\tau = \frac{\sum_i g_i e^{-\Delta E_i/kT}}{\sum_i \frac{g_i}{\tau_i} e^{-\Delta E_i/kT}}, \tag{1}$$

where $i=1-4$ labels the different states counting from lowest energy; g_i is the degeneracy, ΔE_i is the energy difference between the ith level and the lowest-energy level $i=1$ (L_{1A}) and τ_i is the radiative lifetime of the ith state. Motivated by the 6H-SiC Zeeman results (Ref. 7) we use $g_1=2$ and $g_2=g_3=g_4=1$. The upper doublet associated with L_1 is assumed to be slow, and therefore not affecting the lifetime. Using the information from temperature-dependent PL measurements we can reduce the number of remaining free parameters to three: τ_1, τ_2, and ΔE_2. From the temperature dependence of M_1/L_1 and H_1/L_1 we get the oscillator ratios $\tau_2/\tau_3=135$ and $\tau_2/\tau_4=65$, assuming that the main contribution to the L_1 PL intensity is coming from L_{1B}. Furthermore, we have $\Delta E_3=8$ meV and $\Delta E_4=11$ meV. A reasonable fit to the lifetime data is achieved with $\tau_1=550$ μs, $\tau_2=25$ μs, and $\Delta E_2=0.45$ meV (see Fig. 7). The high τ_1/τ_2 ratio agrees with the assumption that the main contribution to the L_1 PL intensity at low temperatures is coming from L_{1B}. The fast component observed at the lowest temperatures has a lifetime τ_B lying close to the value of τ_2 found from the fitting. Its appearance may be explained by the absence of thermal equilibrium between the L_{1A} and L_{1B} states at the lowest temperatures. In order to have thermal equilibrium between the two states the transfer rate between them has to be faster than the fastest recombination rate, which is in this case from the L_{1B} state. If this is not fulfilled, the PL decay will be composed of two components, one coming from the decay of the faster state, the other from the decay of the slower state. The disappearance of the fast component at temperatures above approximately 3 K indicates that the states have become thermalized at this temperature.

D. Photoluminescence excitation spectroscopy

Figure 8 shows part of the PLE spectrum of the D_1 L_1 no-phonon line at 2 K. Several sharp lines appear in the spectra. The lines labeled M_1 and H_1 are the strongest and correspond to the M_1 and H_1 lines observed in PL measurements. This can be seen in Fig. 2(d) where part of the PLE spectrum of the 82.7-meV phonon replica of the L_1 line at 2 K is compared to PL spectra at different temperatures. The small N_1 peak approximately 0.5 meV above M_1 in Fig. 8 and Fig. 2(d) is not observed in PL, probably due to the broader linewidth in that case. As in the case of selectively excited PL we generally observe the R_1, R_2, and R_3 Raman lines in our PLE spectra. However, in the two figures mentioned above the Raman lines lie outside of the regions of the spectra that are shown. PLE spectra taken at different parts of the phonon spectrum are all identical except of course for

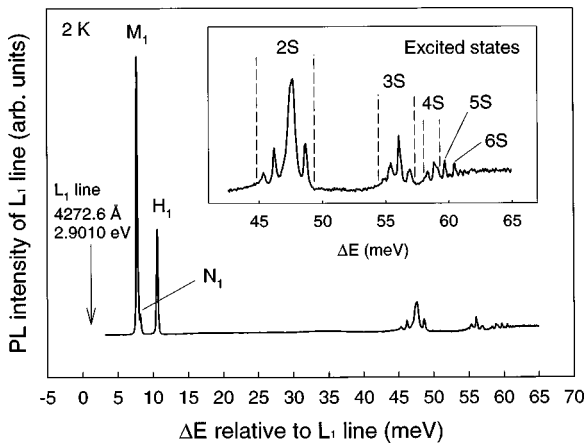

FIG. 8. PLE spectrum of the L_1 line at 2 K. The inset shows a blown up view of the series of sharp lines between 45 and 65 meV above the L_1 line. Tentative assignments to *S*-like hydrogenic states are shown in the inset.

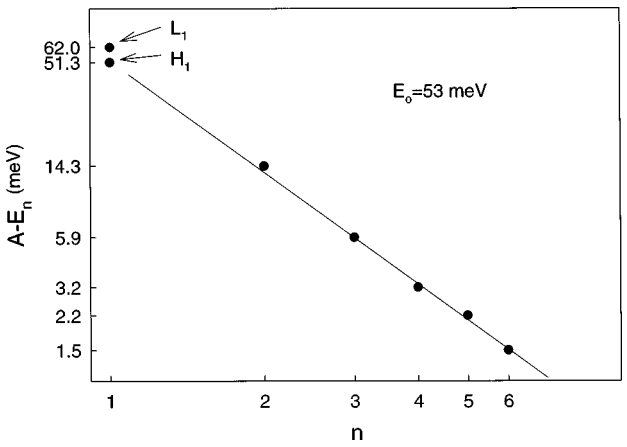

FIG. 9. The figure shows $\ln(A-E_n)$ vs $\ln(n)$. The solid line shows a fit based on Eq. (2) using $A=62$ and $E_0=53$ meV.

the position of the Raman lines. When monitoring within the TO band (see Fig. 1) for instance, the R_1 and R_2 lines are situated close to the M_1 and H_1 lines. We used such spectra to calibrate the M_1 and H_1 line positions using the Raman lines as a reference. In the PLE spectra [see Fig. 2(d)] the L_1 line is very weak compared to the M_1 and H_1 lines, indicating an almost forbidden transition. This agrees well with the temperature-dependent PL where the L_1 line is seen to decrease drastically at higher temperatures when the M_1 and H_1 levels become increasingly thermally populated. The relative oscillator strengths of the no-phonon lines as determined from the PLE spectrum are $M_1/L_1 \sim 140$ and $H_1/L_1 \sim 55$. The values agree approximately with those found from temperature-dependent PL. The phonon assisted part of the PLE spectrum is shown in Fig. 5. The phonon bands are qualitatively similar to those seen in PL, with the exception of the gap modes, which are not seen in the PLE spectrum. According to Dean, Bimberg, and Choyke (Ref. 7), the exchange coupling and crystal field lead to a threefold splitting of the exciton ground state. According to this, there should be only two high-energy lines associated with D_1 excitons. From this we see that both the number of high-energy lines in 4H-SiC, and their polarization contradicts the above model.

An additional series of lines is observed within an energy range between 45 and 65 meV higher than the L_1 no-phonon line. These appear to be composed of groups of lines with the spacing between groups and the spacing between their internal lines as well as the intensity, decreasing as the energy increases. The characteristics of the series of line groups are reminiscent of a hydrogenic series of excited states. The inset of Fig. 8 shows a blown up view of the region where the series of lines appears. For the first two groups from the left we clearly resolve four lines, but for the lines at higher energies the situation is less clear. Our tentative group assignments are shown in the figure ($2S$, $3S$, etc.). The low energy of the excited states as compared to the localization energy of the exciton can be explained by one of the particles being weakly bound by the Coulomb field of the other. Excited states of excitons have been observed before for various defect systems in other semiconductors than SiC. A good example is the series of excited hole states observed with PLE spectroscopy on excitons bound at NN_i pairs in GaP.[19] The ground state of the D_1 exciton is split into four components L_1, M_1, N_1, and H_1. The transitions associated with L_1 and N_1 are weak and we would expect in a first approximation that the same be true for the excited states of the exciton. The selection rule for creation of excitons in a parity allowed transition requires that they be created in *S*-like states.[19] From this we expect *a priori* only *S*-like excited states split at most into two components to show up in the PLE spectra. This obviously contradicts our assignment of four lines to the $2S$ and $3S$ groups (see Fig. 8). The most likely explanation for this discrepancy is the breaking of the parity selection rule. This would, according to effective mass theory, lead to extra lines associated with *P*-like states. For comparison with the simple hydrogenic theory, we use the line positions of the strongest component within each group. We have fitted the following model to our data:

$$A-E_n=\frac{1}{n^2}E_0. \tag{2}$$

Here A is the energy of the series limit, E_n is the measured energy of the nS lines, and E_0 is the hydrogenic ground-state energy. A good fit was obtained for $A=62$ meV above the L_1 line, and $E_0=53$ meV. Figure 9 shows the $\ln(A-E_n)$ versus $\ln(n)$ plot using these values. From the fitting results we conclude that a hydrogenic series describes well our data. From E_0 we can determine the approximate effective mass of the weakly bound particle with the aid of the following formula:

$$E_0=\frac{m^*e^4}{8h^2\varepsilon^2\varepsilon_0^2}, \tag{3}$$

where E_0 is the same as in Eq. (2), m^* is the effective mass, and ε is the dielectric constant. Using $\varepsilon=9.7$ (Ref. 20) and $E_0=53$ meV, we get $m^*=0.37m_0$. According to Optically Detected Cyclotron Resonance measurements the principal values of the electron effective mass tensor in 4H-SiC are $m_{ML}=0.33m_0$, $m_{M\Gamma}=0.58m_0$, and $m_{MK}=0.31m_0$.[21] For *S*-like states that resemble hydrogenic *s* states we assume that the three masses are equally important, and that the effective mass can be estimated by $m_e^*=(m_{M\Gamma}m_{MK}m_{ML})^{1/3}$

$=0.39m_0$. The effective masses of holes in 4*H*-SiC have not been determined experimentally, but recent theoretical calculations give $m_{\parallel}\sim 1.6m_0$ and $m_{\perp}\sim 0.6m_0$.[22] For hydrogenic *s* states this leads to $m_h^*=(m_{\parallel}m_{\perp}m_{\perp})^{1/3}\sim 0.8m_0$. Obviously this comparison favors the electron as the weakly bound particle of the D_1 exciton. However, due to delocalization of the primary particle, the Coulomb binding energy of a secondary particle in an exciton is expected to be less than for a particle bound at an effective mass donor or acceptor. A definite assignment of the weakly bound particle to an electron is therefore not possible at this stage.

The application of photoluminescence excitation spectroscopy to the D_1 center in SiC has to our knowledge only been reported before for the 3*C* and 6*H* polytypes.[8] No information as to how the spectra were measured was given in this report, however, except that they were recorded by using two monochromators, one of which was used for analysis. This means that the other monochromator must have been used in conjunction with some type of lamp for means of excitation. In the PLE spectra of the above-mentioned report there is no sign of any lines that can be attributed to excited states of the excitons. We conclude that our PLE spectra are the first to show evidence for excited states of the D_1 exciton in any polytype of SiC.

IV. SUMMARY AND CONCLUSIONS

At low temperatures the D_1 PL in 4*H*-SiC consists of one no-phonon line L_1 (4272.6 Å) followed by a phonon assisted structure. As the temperature is raised, two higher energy no-phonon lines, M_1 (4261.3 Å) and H_1 (4257.0 Å), appear and the L_1 intensity rapidly decreases. The lines L_1, M_1, and H_1 are all polarized perpendicular to the crystal *c* axis. At sufficiently high temperatures the D_1 PL is quenched. The activation energy is found to be approximately 57 meV. At high temperatures the time decay of the three no-phonon lines L_1, M_1, and H_1 is identical, which shows that they are thermalized. The lifetime at 1.3 K is approximately 450 μs but decreases to a few μs at 70 K. The lifetime changes most rapidly between 1.3 and 4.2 K, and between 15 and 70 K. We attribute the change at low temperature to population effects within closely spaced levels associated with the L_1 state. The change at high temperatures is due to increased population of the M_1 and H_1 states. PL excitation spectra of phonon replicas of the L_1 line at low temperature reveal a weak peak corresponding to the L_1 no-phonon line and two strong peaks corresponding to the M_1 and H_1 lines. We also notice a weak peak, N_1, approximately 0.5 meV above the M_1 line. Furthermore, there is a series of sharp lines at higher energies in the PLE spectra. The energy positions of the lines fit well a hydrogenic series of excited states. The fitting gives a binding energy of 53 meV and an associated effective mass $m^*=0.37m_0$.

The main characteristics of the D_1 bound exciton in 4*H*-SiC are similar to those observed previously for the 3*C* and 6*H* polytypes. The results are consistent with an exciton residing at an isoelectronic center. Certain aspects of our results, such as the polarization of the M_1 and H_1 lines and the observation of the N_1 line in PLE, contradict the *J*-*J* coupling model proposed previously on the basis of Zeeman results for D_1 excitons in 6*H*-SiC.[7] Our investigation gives important new information concerning the structure of the D_1 exciton. The low activation energy of the quenching of the D_1 PL, and the excited states observed in the PLE spectra, show that one of the excitonic particles is weakly bound. The effective mass of the secondary particle, obtained by fitting the PLE results to a simple hydrogenic model, is similar to the electron effective mass in 4*H*-SiC.

ACKNOWLEDGMENTS

We are grateful to J. L. Lindström and U. Forsberg for the sample preparation. Support for this work was provided by the Swedish Council for Engineering Sciences (TFR), the Swedish Foundation for Strategic Research (SSF), and ABB Corporate Research.

*Electronic address: tryeg@ifm.liu.se

[1] W. J. Schaffer, G. H. Negley, K. G. Irvin, and J. W. Palmour, in *Diamond, Silicon Carbide and Nitride Wide Bandgap Semiconductors*, MRS Symposia Proceedings No. 339, edited by C. H. Carter, Jr., G. Gildenblat, S. Nakamura, and R. Nemanich (Materials Research Society, Pittsburgh, 1994), p. 595.

[2] Yu. A. Vodakov and E. N. Mokhov, in *Silicon Carbide—1973*, edited by R. C. Marshall, J. W. Faust, and E. E. Ryan (University of South Carolina Press, Columbia, South Carolina, 1974), p. 508.

[3] W. J. Choyke, in *The Physics and Chemistry of Carbides, Nitrides and Borides*, Vol. 185 of *NATO Advanced Study Institute Series E: Applied Sciences*, edited by Robert Freer (Kluwer Academic, Dordrecht, 1990), p. 563.

[4] W. J. Choyke and L. Patrick, Phys. Rev. B **4**, 1843 (1971).

[5] L. Patrick and W. J. Choyke, Phys. Rev. B **5**, 3253 (1972).

[6] W. J. Choyke and L. Patrick, in *Proceedings of the International Conference on Radiation Damage and Defects in Semiconductors*, IOP Conf. Proc. No. 16 (Institute of Physics and Physical Society, London, 1973), p. 218.

[7] P. J. Dean, D. Bimberg, and W. J. Choyke, in *Proceedings of the International Conference on Defects and Radiation Effects in Semiconductors*, IOP Conf. Proc. No. 46 (Institute of Physics and Physical Society, London, 1979), p. 447.

[8] Y. M. Suleimanov, V. M. Grekhov, K. D. Demakov, and I. V. Plyuto, Sov. Phys. Solid State **27**, 1910 (1985).

[9] P. J. Dean and D. C. Herbert, in *Excitons*, edited by K. Cho, Topics in Current Physics Vol. 14 (Springer-Verlag, Berlin, 1979), p. 55.

[10] W. J. Choyke, in *Proceedings of the International Conference on Radiation Effects in Semiconductors*, IOP Conf. Proc. (Institute of Physics and Physical Society, London, 1977), p. 58.

[11] V. V. Makarov, Sov. Phys. Solid State **13**, 1974 (1972).

[12] Ch. Haberstroh and R. Helbig, J. Appl. Phys. **76**, 509 (1994).

[13] T. Dalibor, C. Peppermuller, G. Pensl, S. Sridhara, R. P. Devaty, W. J. Choyke, A. Itoh, T. Kimoto, and H. Matsunami, in *Proceedings of the Sixth International Conference on Silicon Carbide and Related Materials*, IOP Conf. Proc. No. 142 (Institute of Physics and Physical Society, London, 1996), p. 517.

[14] T. Dalibor, G. Pensl, T. Kimoto, H. Matsunami, S. Srindhara, R. P. Devaty, and W. J. Choyke, Diamond Relat. Mater. **6**, 1333 (1997).

[15] Hiroshi Harima, Shin-ichi Nakashima, and Tomoki Uemura, J. Appl. Phys. **78**, 1996 (1995).
[16] O. Kordina, A. Henry, J. P. Bergman, N. T. Son, W. M. Chen, C. Hallin, and E. Janzén, Appl. Phys. Lett. **66**, 1373 (1995).
[17] G. B. Dubrovskii and V. I. Sankin, Sov. Phys. Solid State **17**, 1847 (1975).
[18] J. J. Hopfield, D. G. Thomas, and R. T. Lynch, Phys. Rev. Lett. **17**, 312 (1966).
[19] E. Cohen and M. D. Sturge, Phys. Rev. B **15**, 1039 (1977).
[20] L. A. Patrick and W. J. Choyke, Phys. Rev. B **2**, 2255 (1970).
[21] D. Volm, B. K. Meyer, D. M. Hofmann, W. M. Chen, N. T. Son, C. Persson, U. Lindefelt, O. Kordina, E. Sörman, A. O. Konstantinov, B. Monemar, and E. Janzén, Phys. Rev. B **53**, 15 409 (1996).
[22] C. Persson and U. Lindefelt, J. Appl. Phys. **82**, 5496 (1997).